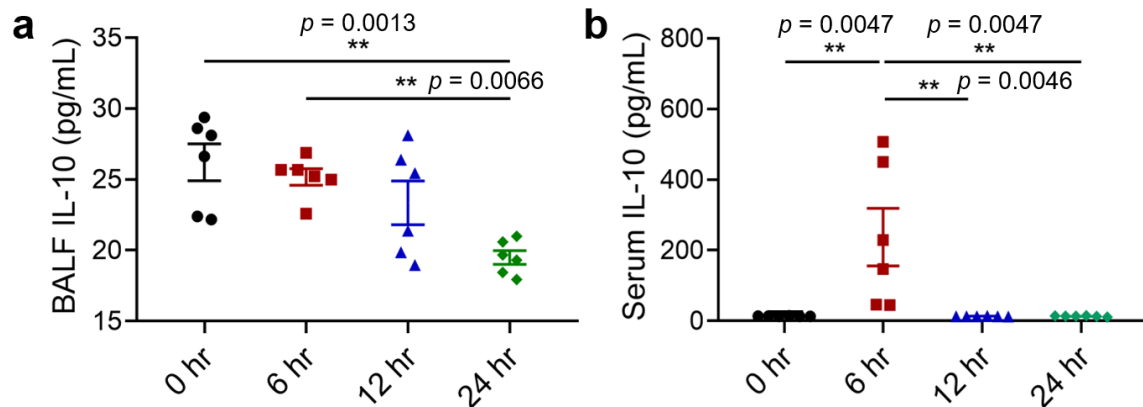
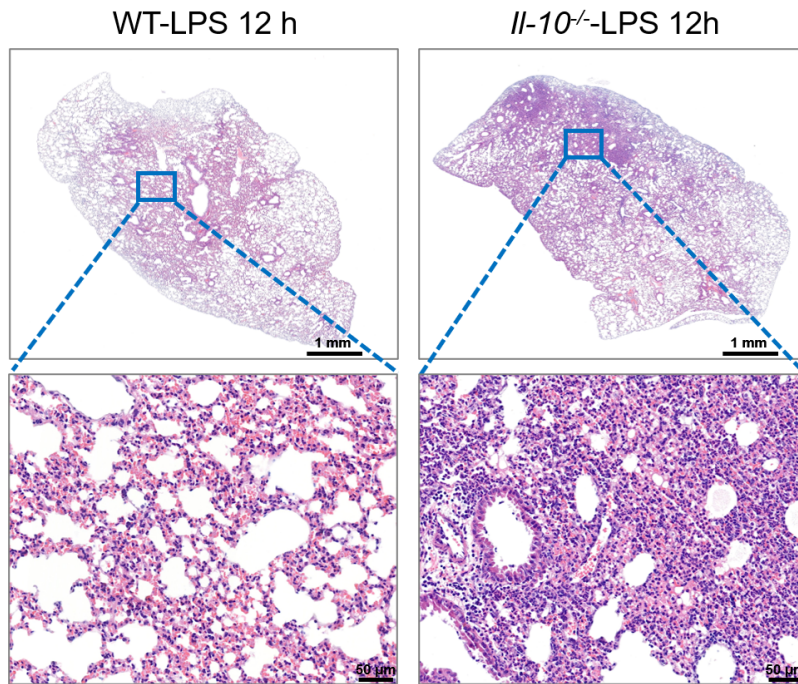


## Supplementary Materials for

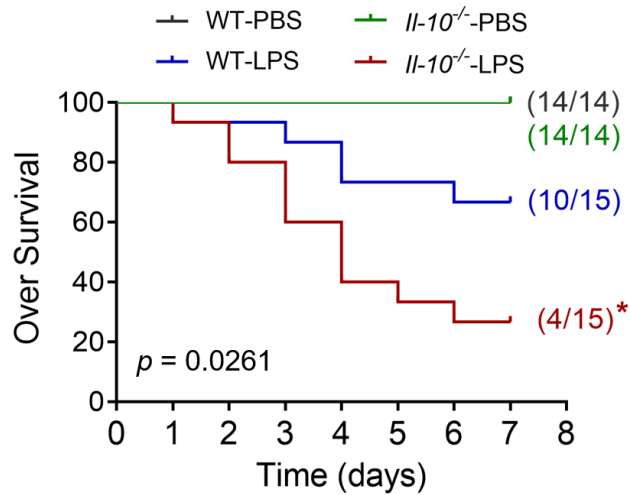
### Locally Orchestrated *Fth1*<sup>hi</sup> Neutrophils Aggravate Inflammation of Acute Lung Injury in an IL-10-Dependent Manner



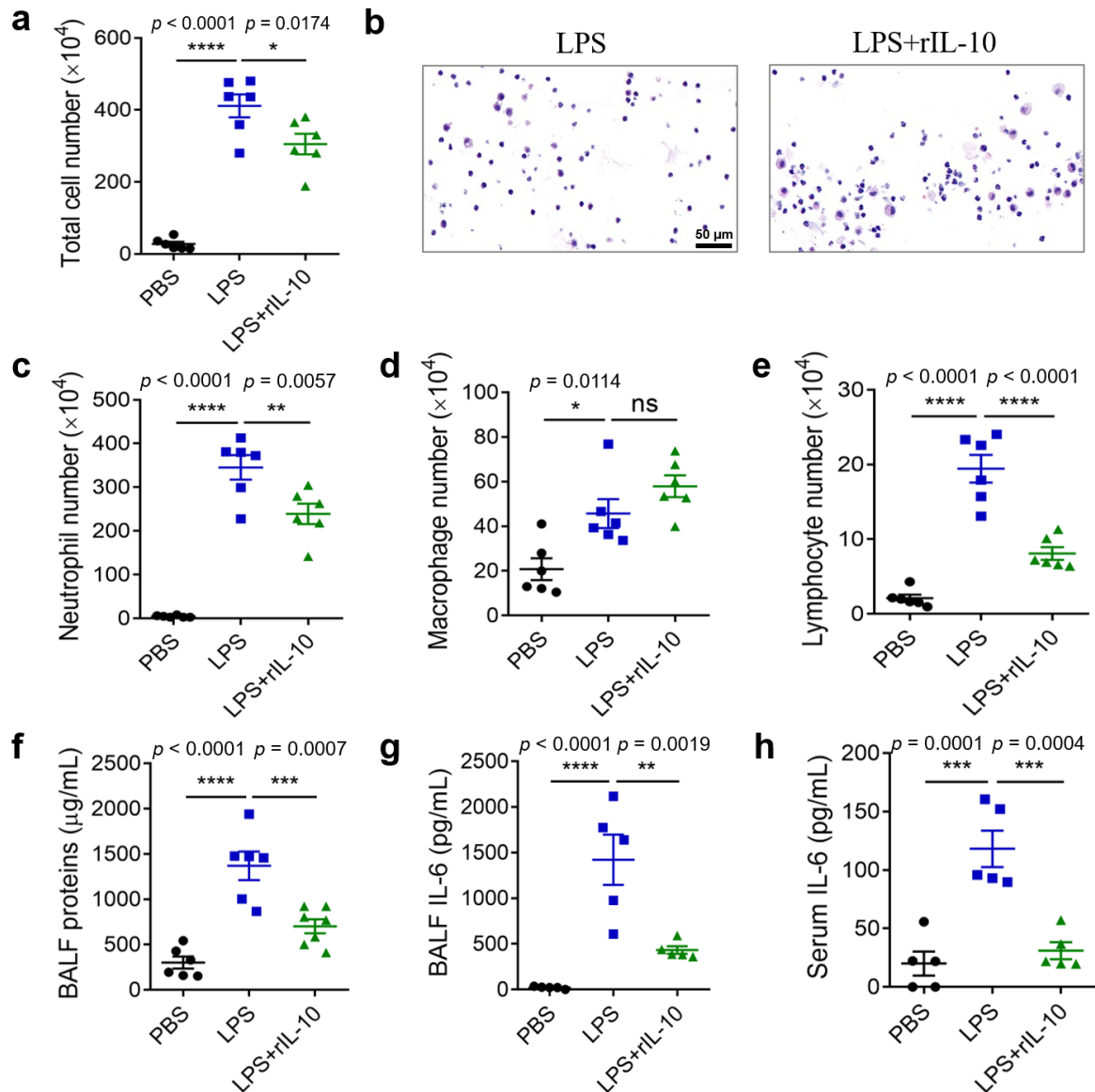
**Supplementary Figure 1. a, b** IL-10 level in BALF supernatant (a) and serum (b) of ALI mice at different time points upon LPS treatment.  $n = 6$  per group. All samples were biologically independent and three or more independent experiments with similar results were performed. Data are presented as mean  $\pm$  SEM and analyzed with a 95% confidence interval. Statistical analysis was performed using one-way ANOVA followed by Bonferroni's post hoc test. Source data are provided as a Source Data file.



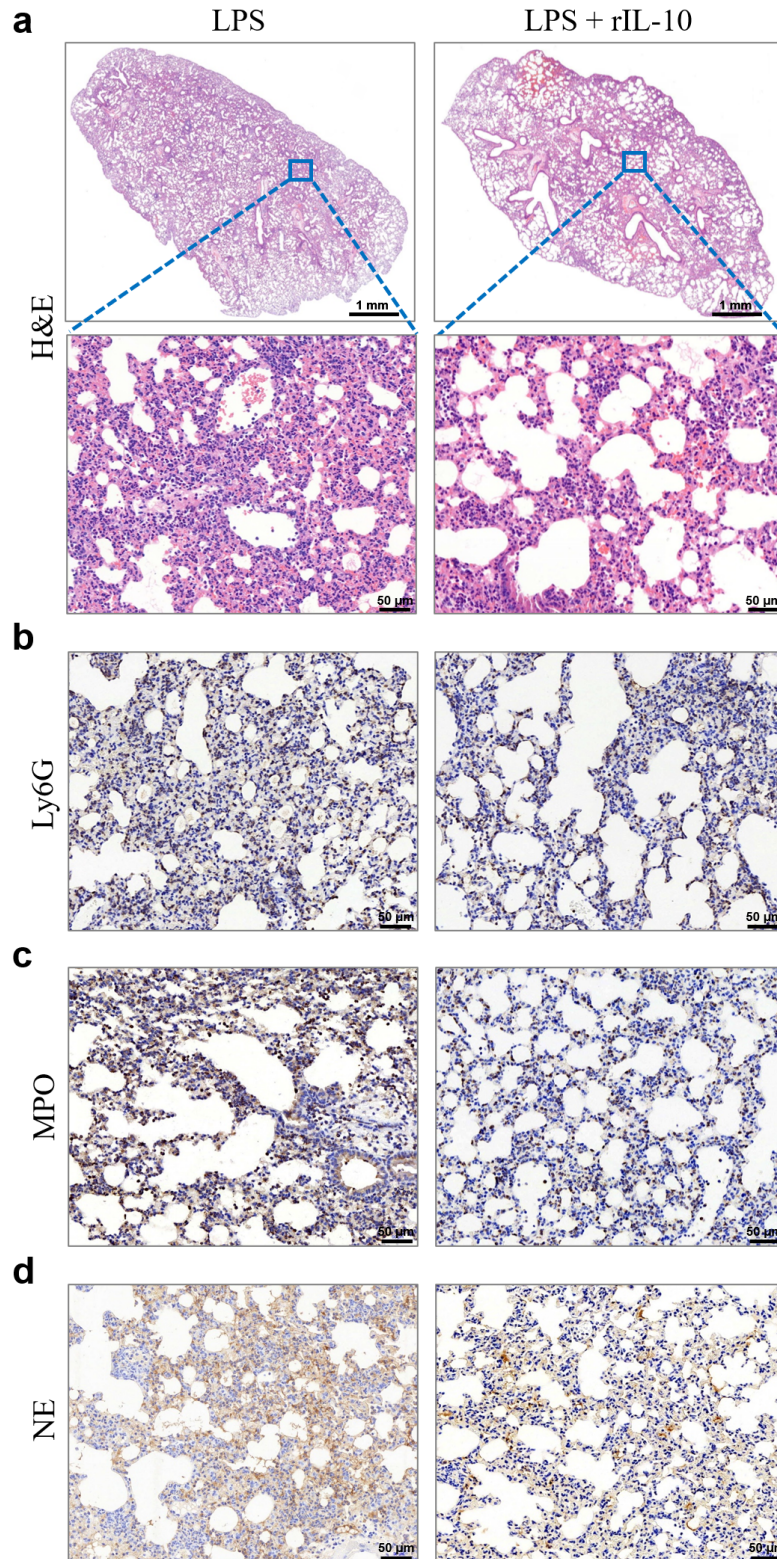
**Supplementary Figure 2.** Representative histological images of H&E-stained lung sections from WT and *Il-10*<sup>-/-</sup> mice at 12 h after LPS inhalation. Scale bars in the upper panel, 1 mm; scale bars in the below panel, 50 μm. Three independent experiments with similar results were performed.



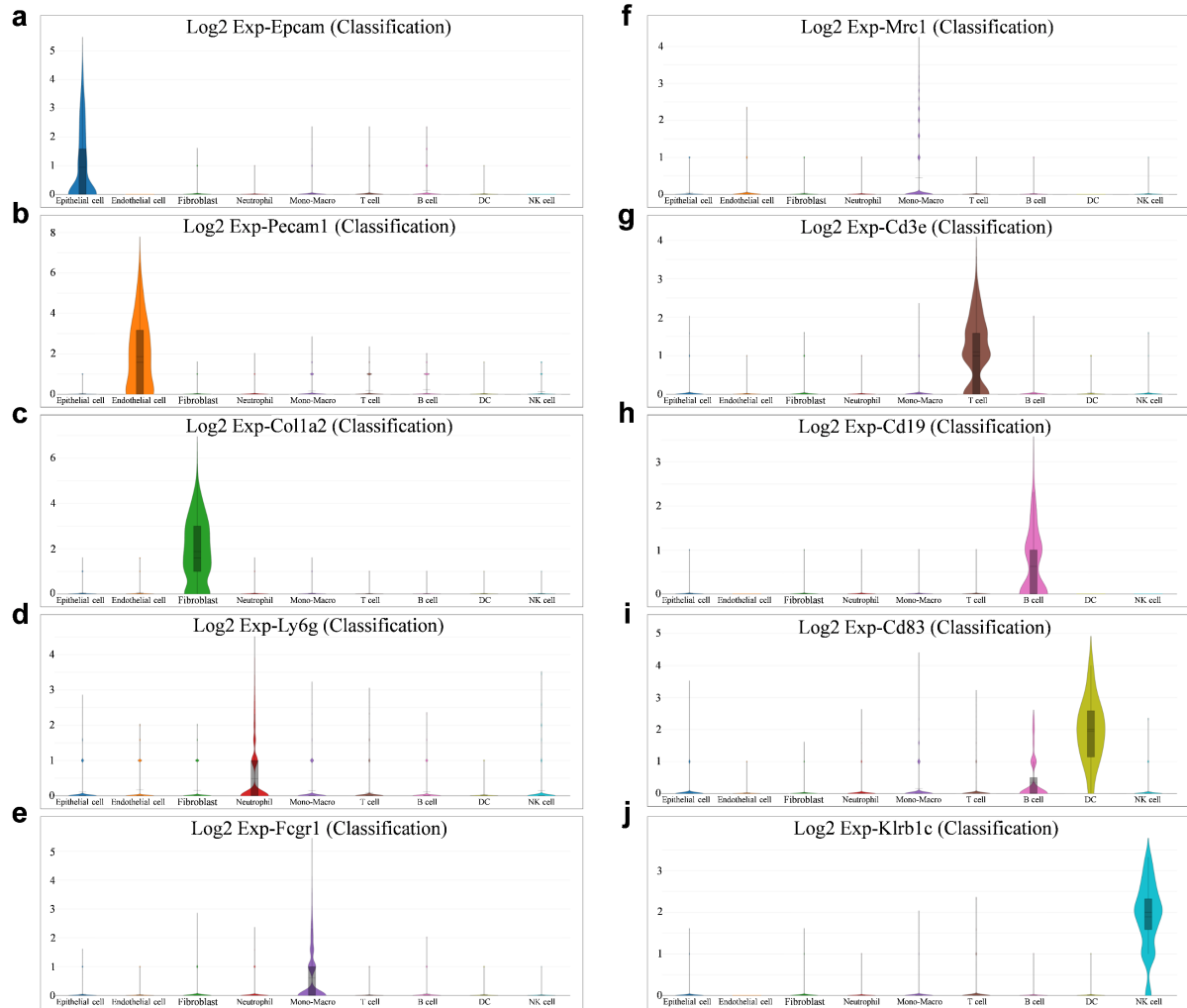
**Supplementary Figure 3.** The effects of *Il-10*<sup>-/-</sup> comparing to WT on survival of the severe ALI mice.  $n = 14, 14, 15, 15$ , respectively in each group. \* $p = 0.0261$  versus WT-LPS group. All samples were biologically independent and three or more independent experiments with similar results were performed. Data are analyzed with a 95% confidence interval. Statistical analysis was performed using Log-rank test. Source data are provided as a Source Data file.



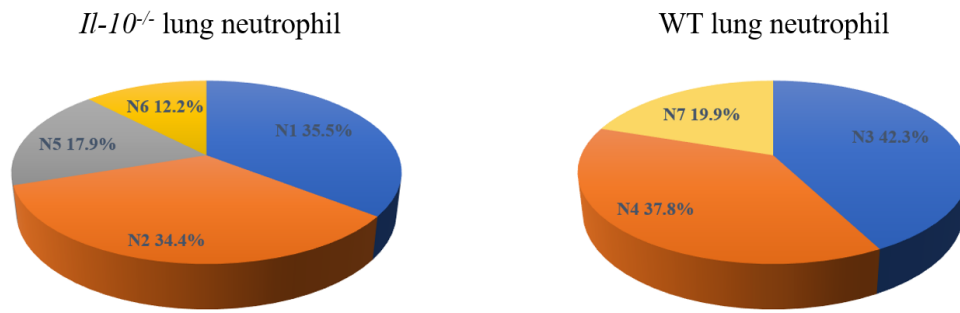
**Supplementary Figure 4.** a-f Mice were co-injected nasally with PBS or recombinant IL-10 (rIL-10; 45  $\mu\text{g/kg}$ ) together with LPS (10  $\text{mg/kg}$ ). Animals were euthanized 24 h after LPS stimulation for the analysis of total cell counts (a,  $n = 6$  per group), H&E staining of cells (b, scale bars, 50  $\mu\text{m}$ ), neutrophil numbers (c,  $n = 6$  per group), macrophage counts (d,  $n = 6$  per group), lymphocyte numbers (e,  $n = 6$  per group) and total protein in BALF (f,  $n = 6, 6, 7$  in each group). g-h Production of IL-6 in BALF (g) and serum (h) is shown,  $n = 5$  per group. ns, not significant. All samples were biologically independent and three or more independent experiments with similar results were performed. Data are presented as mean  $\pm$  SEM and analyzed with a 95% confidence interval. Statistical analysis was performed using one-way ANOVA followed by Bonferroni's post hoc test. Source data are provided as a Source Data file.



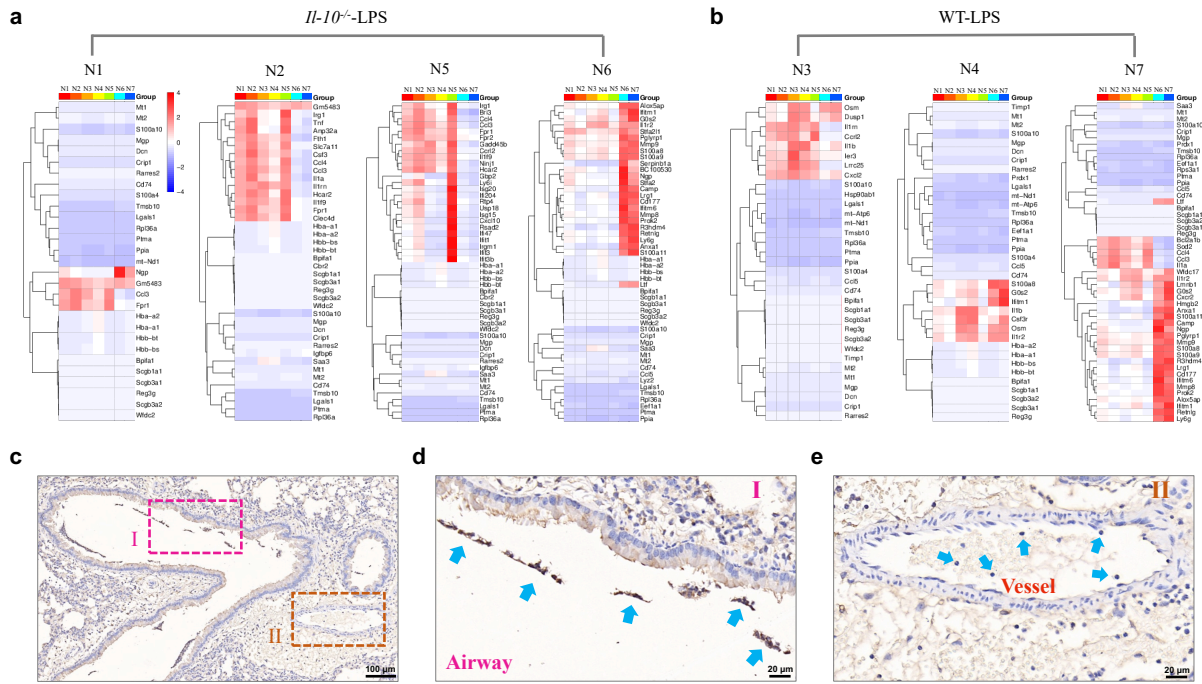
**Supplementary Figure 5.** **a** Representative histological images of H&E-stained lung sections at 24 h after LPS inhalation in the presence or absence of rIL-10 administration. Scale bars in the upper panel, 1 mm; scale bars in the below panel, 50  $\mu$ m. **b-d** Immunohistochemical staining with Ly6G (**b**), MPO (**c**) and NE (**d**) in mouse lung sections. Scale bars, 50  $\mu$ m. Three independent experiments with similar results were performed.



**Supplementary Figure 6. a-j** Violin plots of gene expression in single cells of each population from lungs of WT control, WT LPS-treated and *Il-10*<sup>-/-</sup> LPS-treated mice for described markers in the literature for epithelial cells (a), endothelial cells (b), fibroblasts (c), neutrophils (d), monocyte-macrophages (Mono-Macro) (e, f), lymphocyte T-cells (g), lymphocyte B-cells (h), dendritic cells (DC) (i) and natural killer (NK) cells (j). Boxes within violin plot show the median  $\pm$  1 quartile, with the whiskers extending from the hinge to the smallest or largest value within  $1.5 \times$  interquartile range from the box boundaries.  $n = 469, 168, 683, 7071, 2618, 566, 140, 55, 100$ , respectively.

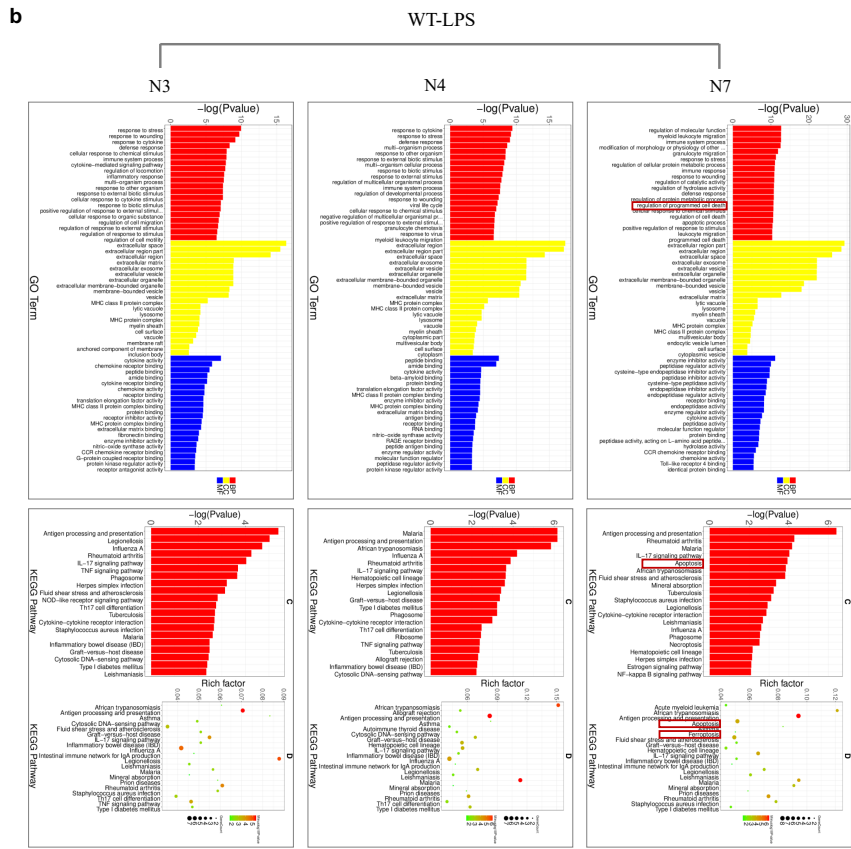
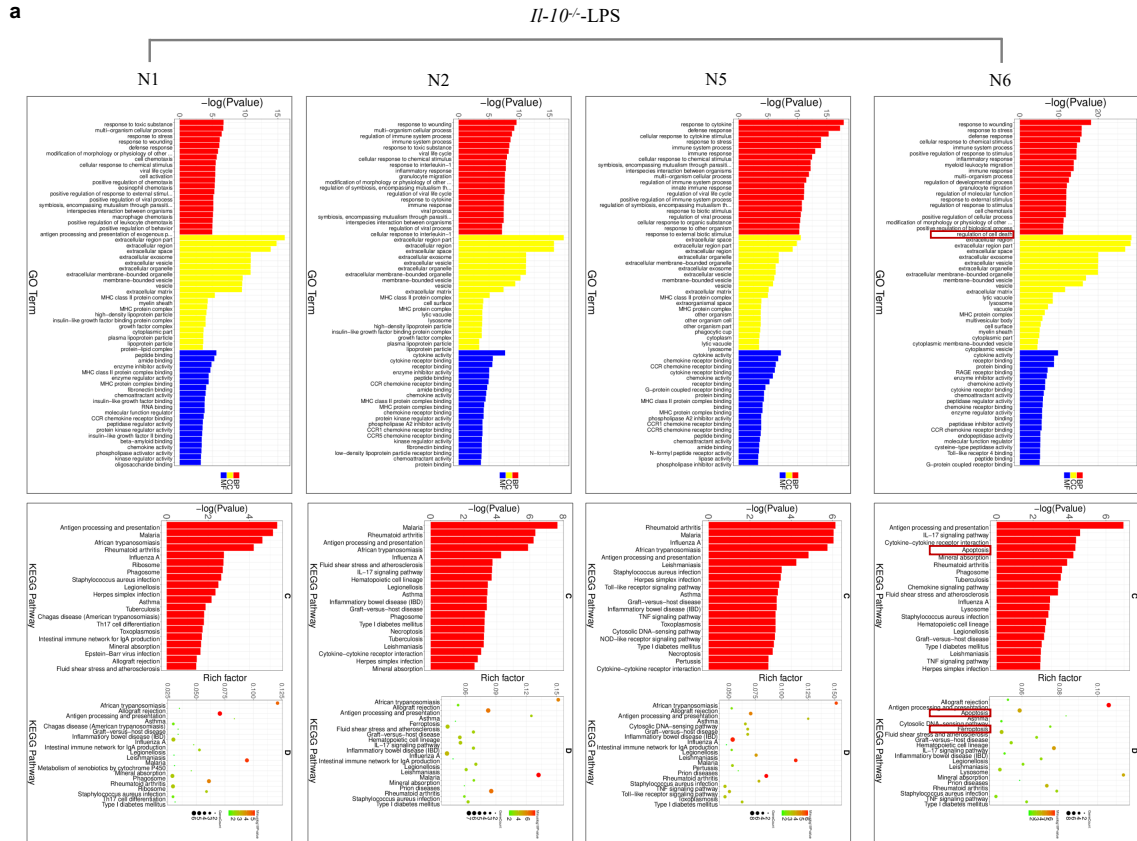


**Supplementary Figure 7.** Proportions of neutrophil populations in lung tissues of *Il-10*<sup>-/-</sup> (left) and WT (right) mouse at 24 h after LPS stimulation.



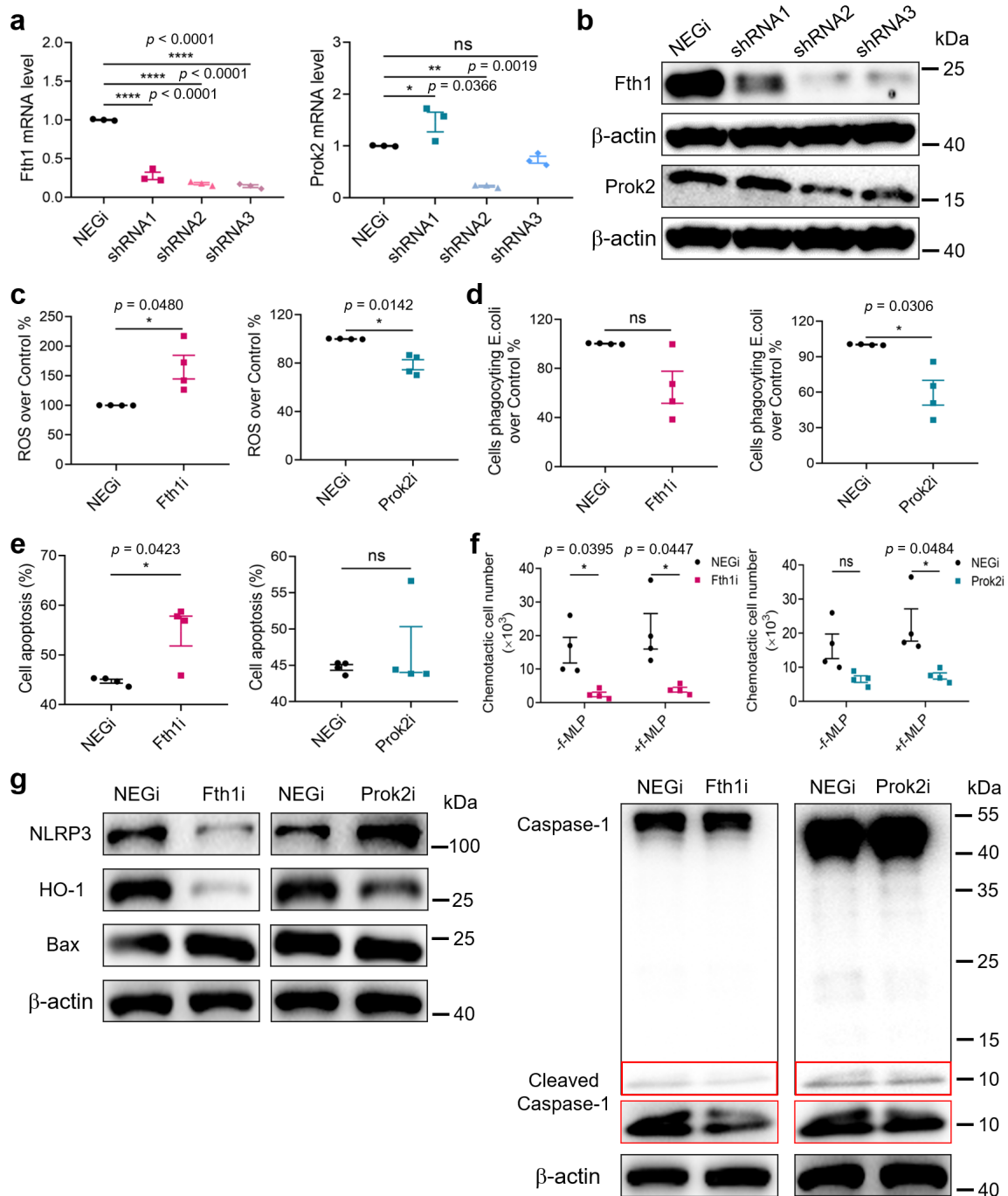
**Supplementary Figure 8.** **a, b** Heatmaps of the top differentially expressed genes in each neutrophil population compared to the others. **c-e** Immunohistochemical staining was performed for Fth1 to determine the distribution of the Fth1<sup>hi</sup> Neu subset in ALI lung tissues. Scale bars, 100  $\mu$ m (**c**); scale bars, 20  $\mu$ m (**d, e**). Blue arrowheads indicate neutrophils in airways (**d**) and pulmonary vessels (**e**). Three independent experiments with similar results were performed.





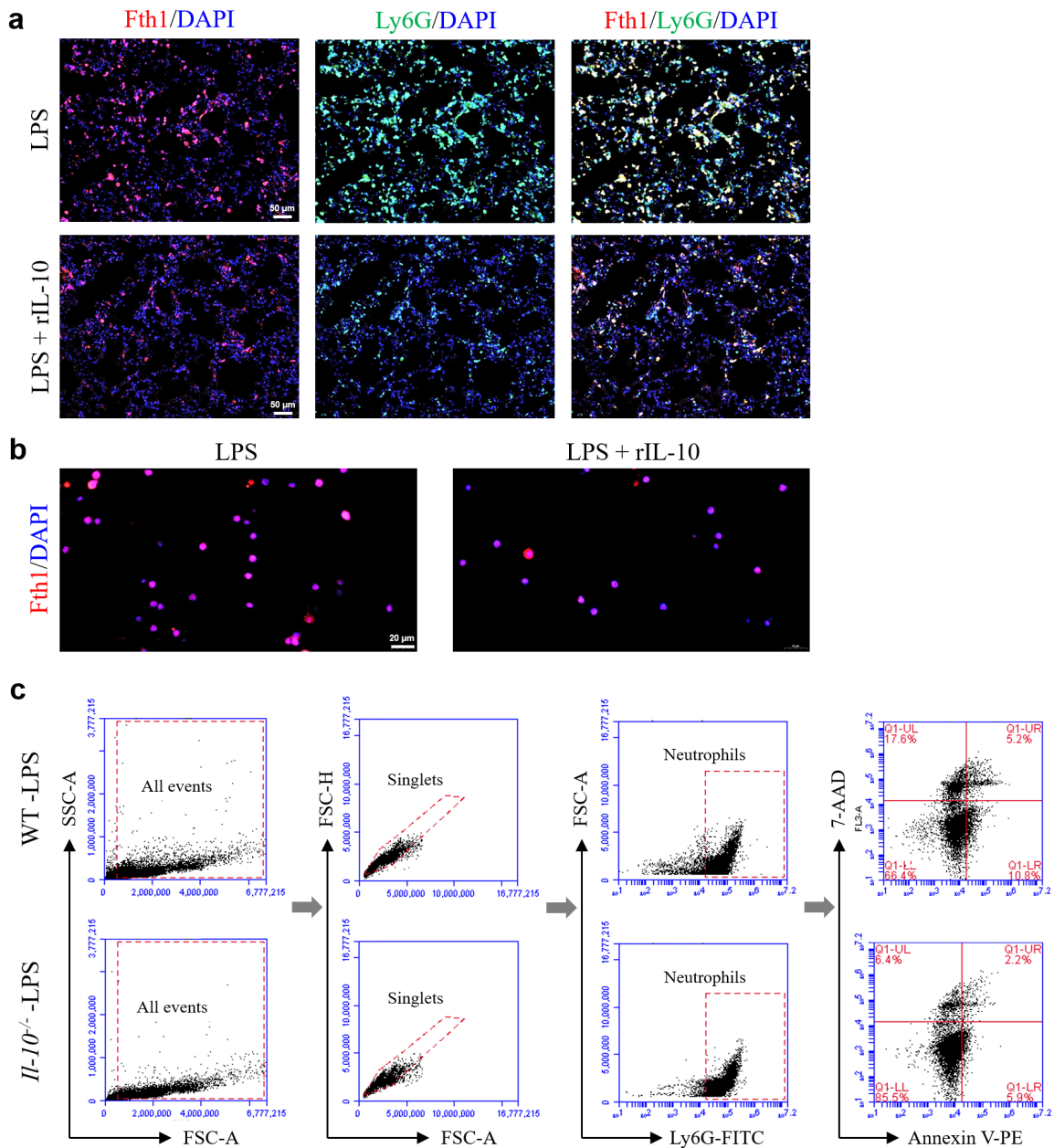
**Supplementary Figure 9. a, b** GO enrichment and KEGG pathway analyses of individual neutrophil subsets in ALI lungs from *Il-10*<sup>-/-</sup> (a) and WT (b) mice. Red boxes indicate the

differential functions between Fth1<sup>hi</sup> (N1-N5) and Prok2<sup>hi</sup> (N6 and N7) neutrophils. The statistical analysis was performed by Fisher's test.

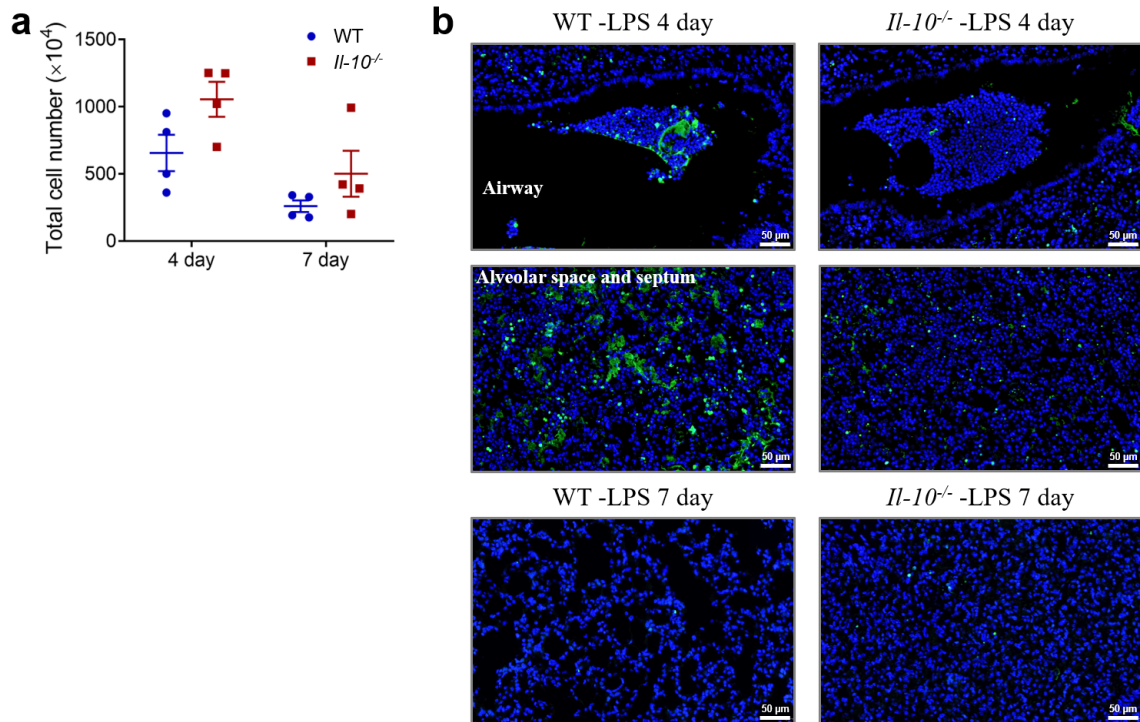


**Supplementary Figure 10.** **a, b** Transfection of human promyelocytic leukemia (HL-60) cells with Fth1/Prok2 shRNA downregulated the mRNA (**a**) and protein (**b**) expression at 12 h compared with control shRNA treatment.  $n = 3$  per group. **c-f** Fth1-depleted neutrophils exhibited function defects in anti-oxidation (**c**), anti-apoptosis (**e**) and chemotaxis (**f**), while Prok2-deficient neutrophils defected in ROS production (**c**), phagocytosis (**d**) and chemotaxis (**f**) of HL-60 cell-derived neutrophils compared with NEGi.  $n = 4$  per group. (**g**) Immunoblotting verifying the effects of Fth1/Prok2 on anti-oxidant HO-1 and pro-apoptotic Bax expression, as well as NLRP3 and cleaved Caspase-1 level for inflammasome activation.

ns, not significant. All samples were biologically independent and three or more independent experiments with similar results were performed. Data are presented as mean  $\pm$  SEM and analyzed with a 95% confidence interval. Statistical analysis was performed using two-tailed unpaired Student t test. Source data are provided as a Source Data file. Uncropped scans of western blot with molecular weight markers were provided in Supplementary Figure 16.



**Supplementary Figure 11.** **a** Representative images of anti-Fth1/anti-Ly6G immunofluorescence-stained lung sections of mice with or without rIL-10 treatment 24 h after LPS challenge. The nuclei were stained with DAPI and are displayed in blue. Scale bars, 50  $\mu$ m. **b** Representative images of anti-Fth1 immunofluorescence-stained airway neutrophils of mice with or without rIL-10 administration 24 h after LPS stimulation. The nuclei were stained with DAPI, displayed in blue. Scale bars, 20  $\mu$ m. Three independent experiments with similar results were performed. **c** Gating strategy and representative scatter plots of BALF cells collected from WT and *Il-10*<sup>-/-</sup> mice at 24 h after LPS challenge. Cellular apoptosis was evaluated by flow cytometry.

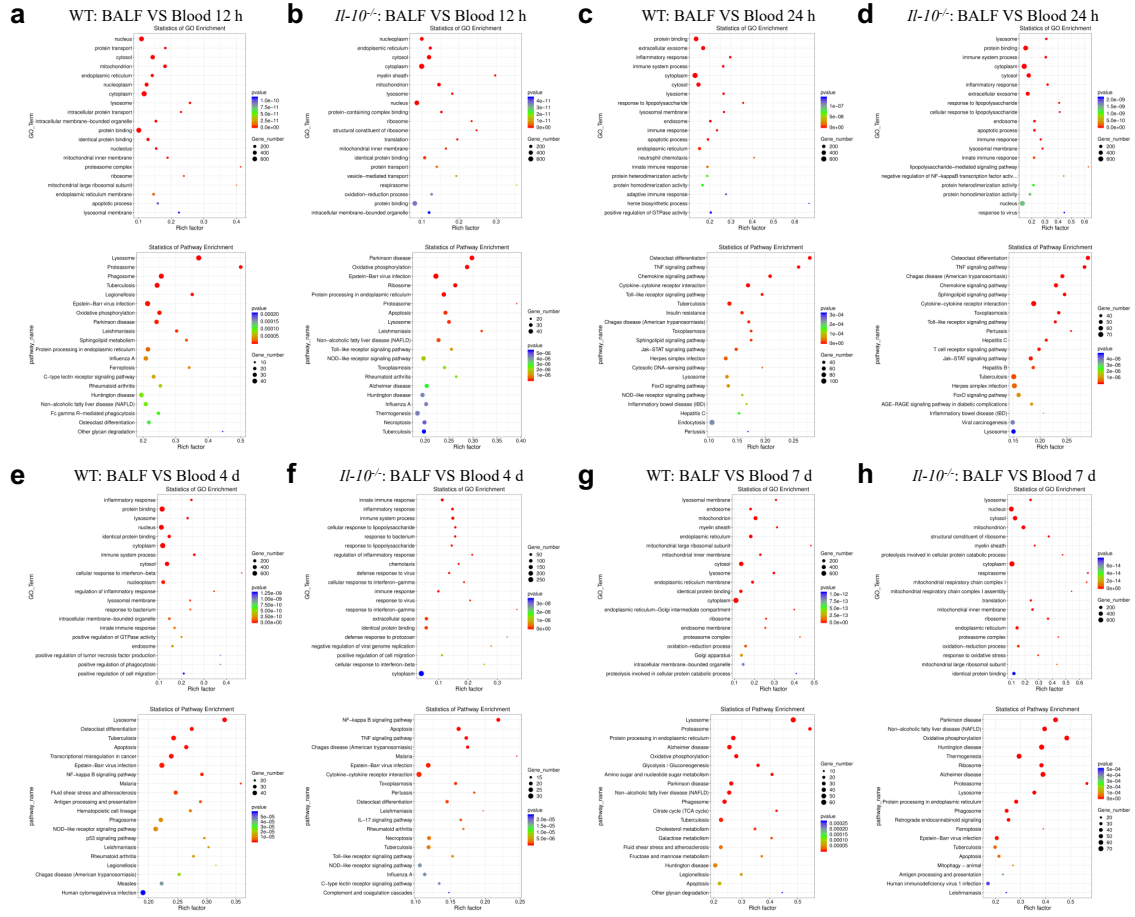


**Supplementary Figure 12.** **a** BALF was collected from WT and *Il-10*<sup>-/-</sup> mice for identifying total counts of inflammatory cells on day 4 and day 7 after LPS challenge,  $n = 4$  in each group. **b** TUNEL staining of apoptotic cells (green) and DAPI staining of nuclei (blue) in lung sections at 4 d and 7 d post-exposure. ns, not significant. All samples were biologically independent and three or more independent experiments with similar results were performed. Data are presented as mean  $\pm$  SEM and analyzed with a 95% confidence interval. Statistical analysis was performed using two-tailed unpaired Student t test. Source data are provided as a Source Data file.

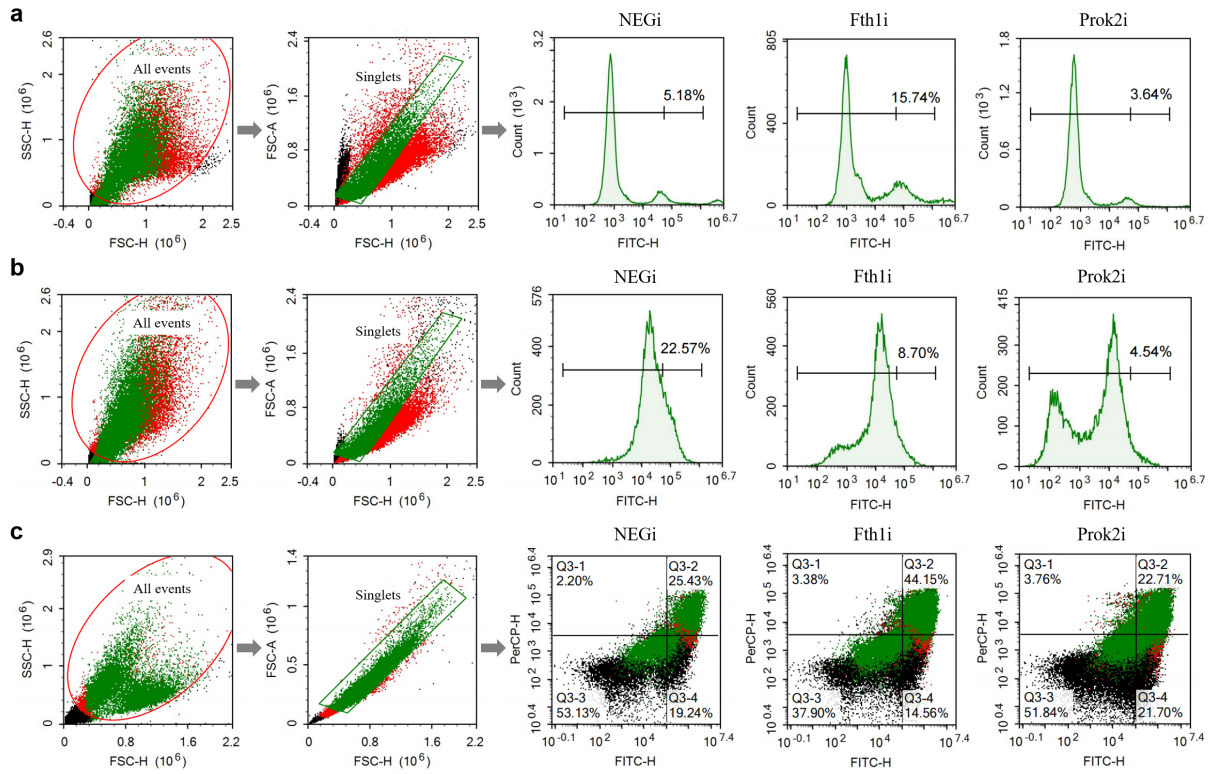


differentially expressed genes in BALF and blood neutrophils from distinct management groups at different time points.  $n = 4$  samples per group. VS, versus.  $p$  values were calculated with a likelihood ratio test between groups.

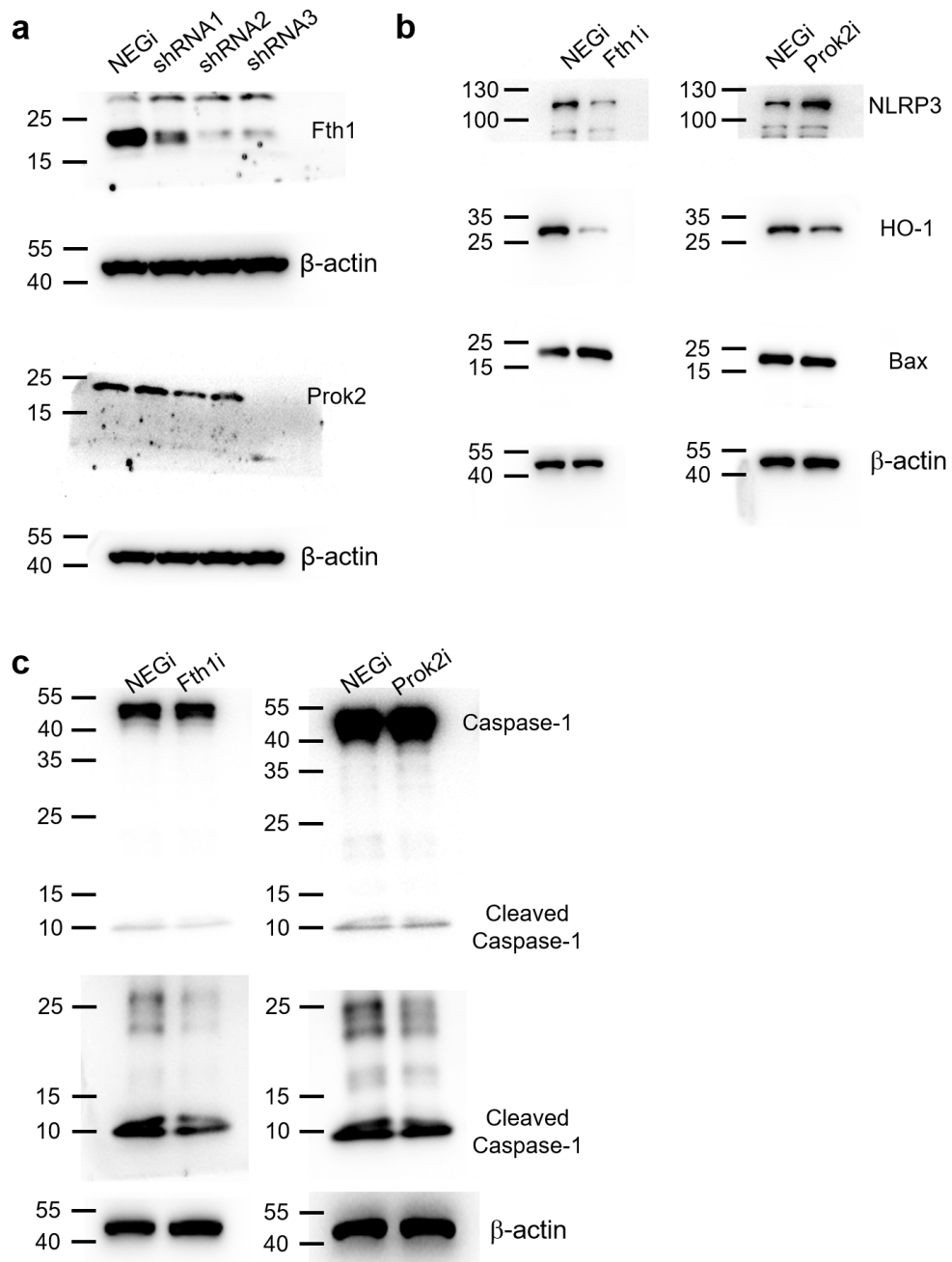




**Supplementary Figure 14. a-h** GO terms and KEGG pathway analyses of BALF and blood neutrophils in different treatment groups at different time points.  $n = 4$  samples per group. VS, versus. The statistical analysis was performed by Fisher's test.



**Supplementary Figure 15. a-c** Gating strategy for the detection of ROS (a), phagocytosis (b) and apoptosis (c) of HL-60 cell-derived neutrophils.



**Supplementary Figure 16.** a-c Uncropped scans of western blot with molecular weight markers, which are related with Supplementary Figure 10.

**Supplementary Table 1: Demographic and clinical characteristics of 24 patients.**

	Age, Yrs, (M, IQR)	Sex	Smoking	Pack-years, Yrs	Cancer history	Current disease	Sample	Underlying diseases					Survival
								Hypertension	Diabetes	Cardiac disease	Autoimmune diseases	Others	
All% or median	67(49-88)	62.50% Male	8.33%	-	16.67%	-		41.67%	12.5%	16.67%	4.17%	50.00%	75.00%
Case 1	49	F <sup>a</sup>	×	-	×			✓	×	✓	×	×	✓
Case 2	54	M <sup>b</sup>	✓	30	×	SP <sup>c</sup> Pneumonia		×	✓	×	×	×	✓
Case 3	66	F	×	-	✓			×	×	×	×	×	✓
Case 4	85	M	×	-	×			×	×	×	×	✓	✓
Case 5	64	F	×	-	×	KP <sup>d</sup>		×	✓	×	×	×	✓
Case 6	64	F	×	-	✓	Pneumonia		✓	×	×	×	×	✓
Case 7	71	M	×	-	✓			×	×	×	×	×	✓
Case 8	73	M	×	-	×			✓	×	×	×	×	✓
Case 9	70	M	×	-	×	HI <sup>e</sup>		×	×	×	×	✓	✓
Case 10	66	M	×	-	×			✓	×	✓	×	×	✓
Case 11	64	F	×	-	✓			×	×	×	×	×	✓
Case 12	54	M	×	-	×	Lung Cancer	BALF	×	×	×	×	✓	✓
Case 13	87	F	×	-	×			×	×	×	×	×	✓
Case 14	61	F	×	-	×	Pulmonary		×	×	×	×	✓	✓
Case 15	72	M	×	-	×	Fibrosis		✓	×	×	×	×	✓
Case 16	67	F	×	-	×			×	×	×	×	✓	✓
Case 17	54	M	✓	30	×	AECOPD <sup>f</sup>		×	×	×	×	✓	✓
Case 18	72	M	×	-	×			✓	×	✓	×	×	×
Case 19	71	M	×	-	×			×	✓	×	✓	✓	×
Case 20	70	F	×	-	×			✓	×	×	×	✓	×
Case 21	65	M	×	-	×	ARDS <sup>g</sup>		×	×	×	×	✓	×
Case 22	66	M	×	-	×			✓	×	×	×	✓	✓
Case 23	88	M	×	-	×			✓	×	×	×	✓	×
Case 24	84	M	×	-	×			✓	×	✓	×	✓	×

<sup>a</sup> F: Female. <sup>b</sup> M: Male. <sup>c</sup> SP: *Streptococcus pneumoniae*. <sup>d</sup> KP: *Klebsiella pneumoniae*. <sup>e</sup> HI: *Haemophilus influenzae*. <sup>f</sup> AECOPD: Acute exacerbation of chronic obstructive pulmonary disease. <sup>g</sup> ARDS: Acute respiratory distress syndrome.